UNIVERSIDADE DE SÃO PAULO

INSTITUTO DE FÍSICA
CAIXA POSTAL 66318
05315-970 SÃO PAULO - SP
BRASIL

PUBLICAÇÕES

IFUSP/P-1254

THE HÉNON-HEILES SYSTEM REVISITED: UNDERSTANDING ITS LARGE STOCHASTIC REGIONS

J.C. Bastos de Figueiredo[1], C. Grotta-Ragazzo[2], C.P. Malta[1]

[1]Instituto de Física, Universidade de São Paulo

[2]Instituto de Matemática e Estatística, Universidade de São Paulo
CP 66281, 05315-970, São Paulo, BRASIL

Janeiro/1997

The Hénon-Heiles system revisited: understanding its large stochastic regions.

J. C. Bastos de Figueiredo[1], C. Grotta Ragazzo[2] and C. P. Malta[1]

[1] *Instituto de Física, Universidade de São Paulo,*

CP 66318, 05315-970, São Paulo-SP, Brasil

[2] *Instituto de Matemática e Estatística, Universidade de São Paulo,*

CP 66281, 05315-970, São Paulo-SP, Brasil

(December 19, 1996)

Abstract

We study the dynamics of a one parameter family of two degrees of freedom Hamiltonian systems that includes the Hénon-Heiles system [1]. We show that several dynamical properties of this family, like the existence of large stochastic regions in the phase space, are related to two canonical invariants that can be explicitly computed. These two invariants characterize universality classes of 2-degrees of freedom Hamiltonian systems with orbits homoclinic (bi-asymptotic) to saddle-center equilibria (related to pairs of real and pure imaginary eigenvalues).

02.30.Hq, 03.20.+i, 05.45.+b, 95.10.Fh, 95.10.Eg

I. INTRODUCTION

Let us consider the one parameter family of Hamiltonian systems related to the following Hamiltonian function

$$H = \frac{1}{2}\left(p_x^2 + p_y^2 + x^2 + y^2\right) + bxy^2 - \frac{y^3}{3} \ . \tag{1}$$

For the parameter $b = 1$ this is a well-known system first studied by Hénon and Heiles [1]. Regardless of the value of $b \geq 0$ this system has, among others, $(x, y, p_x, p_y) = (0, 0, 0, 1) \equiv \eta$ as an equilibrium point. This equilibrium is related to a pair of pure real eigenvalues $\pm\nu = \pm 1$ and a pair of pure imaginary eigenvalues $\pm\omega i = \pm\sqrt{1 + 2b}\, i$. It is said to be of the saddle-center type. The energy of η is $H(\eta) = \frac{1}{6}$. It is called the escape energy because all trajectories starting at $x = y = 0$, with energy $E \leq \frac{1}{6}$, remain bounded, while there are trajectories starting at this same point, with energy $E > \frac{1}{6}$, that are unbounded. System (1) has the invariant plane $(x = 0, y, p_x = 0, p_y)$. On this plane the dynamics is given by the second order equation $\ddot{y} = -y + y^2$. Integrating this equation, we conclude that system (1) has a continuum of periodic orbits Γ_E with energies $E < \frac{1}{6}$ that accumulate on the orbit $\Gamma_{\frac{1}{6}}$ homoclinic to the equilibrium η. The orbit $\Gamma_{\frac{1}{6}}$ is given by $x = p_x = 0$, $p_y = \dot{y}$, $y = 1 - \frac{3}{2}\mathrm{sech}^2(\frac{t}{2})$, and its energy is $\frac{1}{6}$. The idea of this paper is to study system (1) through the map f of first return (or Poincaré map) to a surface section Σ (or Poincaré section) transversal to the family Γ_E, given by $\Sigma = \{(x, y = 0, p_x, p_y > 0)\}$. As usual, it is convenient to use the conservation of energy, and to consider a one parameter family of Poincaré maps, $f_E : \Sigma_E \to \Sigma_E$, where Σ_E denotes the restriction of Σ to the energy level E. For each E, we can use $p_y = \sqrt{2E - p_x^2 - x^2}$ and take x, p_x, with $2E - p_x^2 - x^2 > 0$, as coordinates on Σ_E. Notice that the sections Σ_E that we are using are different from those used by Hénon and Heiles, and others. Their section is defined imposing $x = 0, p_x > 0$, and p_y, y are used as coordinates.

The reason for choosing a different section is that, for $0 \leq E \leq \frac{1}{6}$, the point $(x, p_x) = (0, 0) \stackrel{\text{def}}{=} 0$ is a fixed point of f_E. For $E < \frac{1}{6}$ this fixed point corresponds to the periodic

orbit Γ_E. The map can be locally approximated by its derivative at $\underline{0}$, which, in particular, determines the stability of $\underline{0}$. For $E = \frac{1}{6}$ the point $\underline{0}$ represents the homoclinic orbit $\Gamma_{\frac{1}{6}}$. The map $f_{\frac{1}{6}}$ is not differentiable at this point and no linear approximation can be made. In this case, it has been shown by Lerman [2] and Mielke et al. [3] (see also [4,5]) that the dynamics of $f_{\frac{1}{6}}$ near $\underline{0}$ is approximately given by a map that is continuous but not differentiable at $\underline{0}$. Moreover, these authors showed that, for $|E - \frac{1}{6}|$ and $||(x, p_x)|| \stackrel{\text{def}}{=} ||z||$ sufficiently small, f_E can be approximately given by the following family of maps (see [5])

$$F_E(z) = AR\left[c - \gamma \ln\left|\frac{\omega||z||^2}{2} - (E - \frac{1}{6})\right|\right] z \ , \tag{2}$$

where: $z = (x, p_x) \in \mathbb{R}^2$, with $||z|| > \sqrt{\frac{2}{\omega}(E - \frac{1}{6})}$ for $E > \frac{1}{6}$, and $F_{\frac{1}{6}}(\underline{0}) \stackrel{\text{def}}{=} \underline{0}$ for $E = \frac{1}{6}$, c is some constant, $\gamma \stackrel{\text{def}}{=} \frac{\omega}{\nu} = \sqrt{1 + 2b}$, and

$$R(\theta) \stackrel{\text{def}}{=} \begin{pmatrix} \cos\theta & -\sin\theta \\ \sin\theta & \cos\theta \end{pmatrix}, \quad A \stackrel{\text{def}}{=} \begin{pmatrix} \alpha & 0 \\ 0 & 1/\alpha \end{pmatrix}.$$

The number $\alpha \geq 1$ is obtained from a scattering problem (similar to that appearing in 1-dimension Quantum Mechanics) given by the (x, p_x) components of the equations of motion linearized on $\Gamma_{\frac{1}{6}}$ (see [6,7]). In this case, using the procedure presented in [6,7], it can be shown that

$$\alpha = B + \sqrt{B^2 + 1} \ , \text{where} \tag{3}$$

$$|B| = \left|\frac{\cos(\frac{\pi}{2}\sqrt{1 - 48b})}{\sinh(2\pi\sqrt{1 + 2b})}\right| \text{ or } |B| = \left|\frac{\cosh(\frac{\pi}{2}\sqrt{48b - 1})}{\sinh(2\pi\sqrt{1 + 2b})}\right|,$$

for $b \leq \frac{1}{48}$ or $b > \frac{1}{48}$, respectively. The only unknown coefficient in (2) is the constant c. It does not play an important role in the dynamics topology of F_E (it can be removed by rescaling z and E appropriately).

There exist several well-known mathematical results on the dynamics of F_E and f_E (see [8,2,3,6,4,5]). Here we shall mention only some of them. For $E = \frac{1}{6}$, $F_{\frac{1}{6}}$ presents a remarkable symmetry [4]: it is invariant under discrete dilations $z \to e^{\pi/\gamma} z$ (namely,

$F_{\frac{1}{6}}(e^{\pi/\gamma} z) = e^{\pi/\gamma} F_{\frac{1}{6}}(z)$). This implies that the dynamics of $F_{\frac{1}{6}}$ is self-similar in the sense that it is the same in every annulus given by $e^{k\pi/\gamma} \leq ||z|| < e^{(k+1)\pi/\gamma}$, $k \in \mathbb{Z}$. For $\alpha > 1$, $F_{\frac{1}{6}}$ has a hyperbolic fixed point p distinct from $\underline{0}$. The dilation symmetry then implies that $F_{\frac{1}{6}}$ has an infinite family of fixed points given by $e^{k\pi/\gamma} p$, $k \in \mathbb{Z}$. In [5] it was proved that if $\gamma(\alpha - \alpha^{-1}) > 1$ then the unstable manifold of p intersects transversally the stable manifold of $e^{\pi/\gamma} p$. This and the dilation symmetry imply that the unstable manifold of $e^{k\pi/\gamma} p$ intersects transversally the stable manifold of $e^{(k+1)\pi/\gamma} p$ for all $k \in \mathbb{Z}$, therefore $F_{\frac{1}{6}}$ contains an infinite heteroclinic chain, or "Arnold's transition chain" [9], that connects $\underline{0}$ to infinite. We remark that this transition chain is intimately related to the so called "resonance overlap criterium" of Chirikov [9]. Indeed, the dilation symmetry of F_E can be used to show that if there is an overlap between two adjacent resonance zones, related by the scale factor $e^{\pi/\gamma}$, then all resonance zones of F_E will overlap.

A numerical study of $F_{\frac{1}{6}}$ (equation (2)), presented in [7], has shown that there exists a critical curve in the (γ, α) parameter space, approximately given by $\gamma(\alpha - \alpha^{-1}) = 1/\sqrt{2}$, such that if (γ, α) is below this curve, then there are invariant curves encircling $\underline{0}$; if (γ, α) is above this curve, then the transition chain, mentioned above, exists and no invariant curve encircling $\underline{0}$ can exist. In particular, if (γ, α) is below (above) the critical curve, then $\underline{0}$ is a stable (unstable) fixed point of $F_{\frac{1}{6}}$. In [5] it was rigorously shown that if α is sufficiently close to one, then, for every $\delta > 0$, it is possible to find $\Delta > 0$ such that, for all $E \in [\frac{1}{6} - \Delta, \frac{1}{6} + \Delta]$, both F_E and f_E have an invariant curve around $\underline{0}$ with diameter smaller than δ. The numerical simulations of [7] and of this work suggest that the condition *"α is sufficiently close to one"* in the above statement may be replaced by *"(γ, α) is below the critical curve"*. In [5] it was also shown that if $F_{\frac{1}{6}}$ has the transition chains mentioned above, then the same is valid for $f_{\frac{1}{6}}$.

The goal of this paper is to understand the dynamics of the family of systems (1) near the escape energy $\frac{1}{6}$, by comparing the numerical results of (1) and (2). Our main conclusion is that the existence of large stochastic regions in the Poincaré maps exhibited by Hénon and

Heiles [1] is a consequence of the existence of the infinite transition chain mentioned above. Moreover, for energies close to $\frac{1}{6}$, we can predict the existence or non-existence of a large stochastic region by using the property that there exist critical values γ_c, α_c such that the properties of $F_{\frac{1}{6}}$ change drastically when the critical curve $\gamma_c(\alpha_c - \alpha_c^{-1})$ is crossed. Using the number $\gamma(\alpha - \alpha^{-1})$ we can also predict whether solutions with energy $E > \frac{1}{6}$ escape or not from a certain bounded region of the phase space. This problem has been studied recently by Contopoulos *et al* [10], and our results can partially explain their numerical results on the properties of escaping. In the next section we present our numerical results, followed by the conclusions.

II. NUMERICAL RESULTS

In the following we present numerical results for iterations of the Poincaré map (1st return map) f_E related to (1), as defined in the previous section, and for the map F_E defined in (2). The number $c = 3.582$ in F_E was chosen so as to have one particular bifurcation of $\underline{0}$ occurring at the same value of E for both F_E and f_E.

In Figure 1 we show iterations of f_E (top) and F_E (bottom) for $b = 1$ (Hénon-Heiles system) and for three values of E, $E = \frac{1}{6}, 0.14, 0.12$. We can see that the closer the energy is to $\frac{1}{6}$, the better is the agreement between f_E and F_E. Figure 1 shows that, for $E = \frac{1}{6}$, the topology of both maps is similar up to a radius $||z|| \approx 0.2$, which is approximately fourty percent of the maximum possible radius of $||z|| = \sqrt{2}$. As the energy decreases, the radius of agreement decreases, and at $E = 0.09$ f_E, and F_E, exhibit similar topology only for $||z|| \leq 0.1$.

From Figure 1 it is evident the self-similarity of the iterates of f_E near $\underline{0}$. The scaling factor agrees with the scaling factor of F_E which is given by $e^{\pi/\gamma}$, where $\gamma = \sqrt{3}$.

Using the value of c above, we obtained an excellent agreement between the sequence of bifurcations of f_E, and of F_E, at $\underline{0}$, as E is varied from $\frac{1}{6}$ to 0.09. From the expression (2) for F_E, it is easy to see that, as $E \to (\frac{1}{6})_-$, the linear stability of $\underline{0}$ changes infinitely many

times from elliptic to hyperbolic, and vice-versa. The same is true of f_E (this result was first presented in [11]).

Using the approximate critical curve of $F_{\frac{1}{6}}$, $\gamma(\alpha - \alpha^{-1}) = 1/\sqrt{2}$, and the explicit formulas for γ and α as function of b (see (2) and (3)), we were able to predict that the fixed point $\underline{0}$ of $F_{\frac{1}{6}}$ would loose stability at values of γ and α corresponding to $b \approx 0.49$. A careful numerical analysis of the dynamics of F_E has shown that, in this case, the transition to instability occurs at values γ_c and α_c corresponding to $b = 0.43$. These critical values obtained numerically are such that $\gamma_c(\alpha_c - \alpha_c^{-1}) = 0.55 < 1/\sqrt{2}$, in agreement with the remark in [7] that the approximate critical curve, $\gamma(\alpha - \alpha^{-1}) = 1/\sqrt{2}$, is overestimated. It is remarkable that, under iterations of $f_{\frac{1}{6}}$, $\underline{0}$ undergoes a stability-instability transition also at $b = 0.43$. In Figure 2 we show iterations of $f_{\frac{1}{6}}$ and $F_{\frac{1}{6}}$ for $b = 0.40$ and $b = 0.48$. Again, the self-similarity of the figures near $\underline{0}$ is excellent. This sequence of figures shows that the existence of large stochastic regions in (1) is related to the existence of the already mentioned transition chain, and to the fact that $\gamma(\alpha + \alpha^{-1}) > 1/\sqrt{2}$.

Orbits of (1) that start on Σ with $E > \frac{1}{6}$ and $||z||^2 \leq \frac{2E}{\omega}$ can escape over the saddle point of the potential of the Hamiltonian (1) and become unbounded. These escaping orbits correspond approximately to the set of points z satisfying $||F_E(z)||^2 < \frac{2}{\omega}(E - \frac{1}{6})$. Using the results in [5] and [7], we were lead to the conjecture that the above mentioned invariant circles exist for (γ, α) below this critical value of F_E or, correspondingly, for $b < 0.43$ in the case of f_E. Our conjecture is fully supported by our numerical results. In Figure 3 we show two sets of iterations of f_E, for $E = 0.17$ and $b = 0.40, 0.48, 1.0$. We considered initial conditions on radii at intervals of 45 degrees. The iteration starts at the origin and many initial conditions were required to obtain the Poincaré sections displayed in Figure 3. The iterations that (do not) escape are represented by black (grey) dots. Points falling inside the central white circle escape immediatly. In the Poincaré section for $b = 0.40$ we can see an invariant grey circle enclosing the black dots. These invariant circles are destroyed in the case $b = .48$. In the case $b = 1.0$ all of the initial conditions used by us escaped.

III. CONCLUSION

Our important conclusion is that the dynamics of the maps F_E and f_E agree very well for E not far from $\frac{1}{6}$ and z not far from $\underline{0}$. This implies that, in this region, the dynamics of f_E, and therefore of (1), can be characterized by the two invariants, γ and α, related to the equilibrium η, and to the homoclinic orbit $\Gamma_{\frac{1}{6}}$, respectively. Our numerical investigation has shown that the dynamical properties of (1) changes a lot depending on whether b is above or below a critical value, b_c, corresponding to (γ_c, α_c) such that $\gamma_c(\alpha_c - \alpha_c^{-1})$ is close to the (overestimated) approximate value $1/\sqrt{2}$ obtained in [7]. This is the reason for system (1) exhibiting large stochastic regions for energies close to $\frac{1}{6}$, and for the existence of large sets of non-escaping orbits for energies larger than $\frac{1}{6}$. In the particular case of the Hénon-Heiles system ((1) with $b = 1.0$), $\gamma(\alpha - \alpha^{-1}) = 3.09$ explaining the existence of the observed large stochastic regions for E close to $\frac{1}{6}$, and of the small non-escaping region for $E > \frac{1}{6}$. It should be remarked that there is a theorem in [5] that proves the existence of transition chains in (1) if $\gamma(\alpha - \alpha^{-1}) > 1$, which is in agreement with the properties exhibited by the Hénon-Heiles system.

Concluding we assert that the map F_E (equation (2)is universal in the sense that any Hamiltonian system [2–5] with two degrees of freedom, and having solutions homoclinic to saddle-center equilibrium points, can be described by F_E in a neighbourhood of the homoclinic orbit. The numbers α and γ determine the universality classes of these Hamiltonian systems.

ACKNOWLEDGMENTS

JCBF is fully and CPM is partially supported by CNPq (the Brazilian Research Council).

REFERENCES

[1] M. Hénon and C. Heiles, Astron. J. **69**, 73 (1964).

[2] L. M. Lerman, Sel. Math. Sov. **10**, 297 (1991).

[3] A. Mielke, P. Holmes and O. O'Reilly, J. Dyn. Diff. Eqns. **4**, 95 (1992).

[4] C. Grotta Ragazzo, to appear in Comm. Pure Appl. Math. (1997).

[5] C. Grotta Ragazzo, to appear in Comm. Math. Phys. (1997).

[6] C. Grotta Ragazzo, Comm. Math. Phys. **166**, 255 (1994).

[7] C. Grotta Ragazzo, Submmited (1996).

[8] R. C. Churchill and D. L. Rod, J. Diff. Eqns. **37**, 351 (1980).

[9] B. V. Chirikov, Phys. Reports **52**, 264 (1979).

[10] G.Contopoulos and D. Kaufmann, Astron. Astrophys. **253**, 379 (1992); G. Contopoulos, H. E. Kandrup and D. Kauffmann, Physica D **64**, 310 (1993); C. V. Siopis, H. E. Kandrup, G. Contopoulos, and R. Dvorak, "Universal properties of escape", preprint 1996.

[11] R. C. Churchill, G. Pecelli and D. L. Rod , Arch. Rat. Mech. Anal. **73**, 313 (1980).

FIGURES

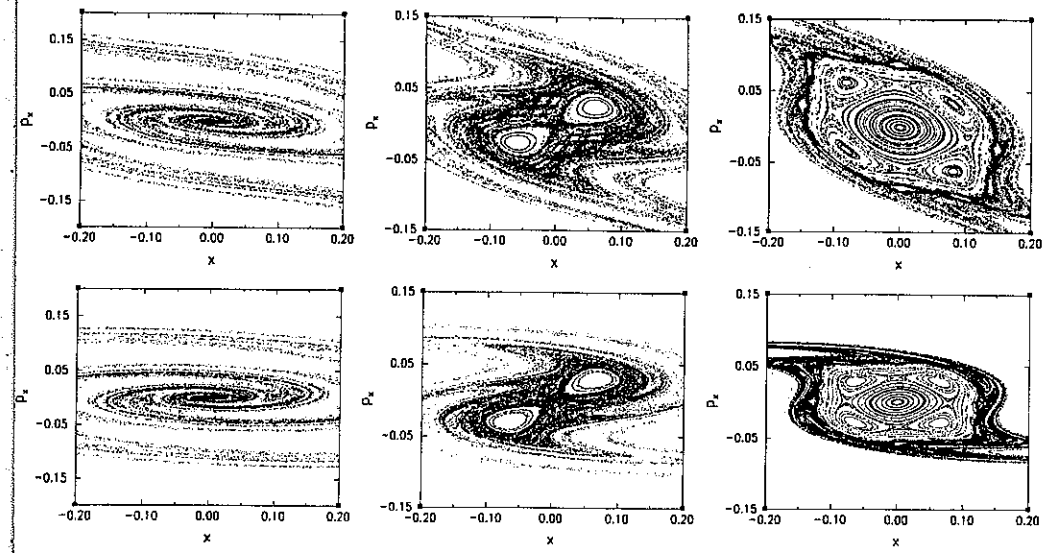

FIG. 1. Poincaré sections of f_E (F_E) are shown on the top (bottom). Energy is $0.1666666667, 0.14, 0.12$ from left to right. Initial conditions are taken on the axes x and p_x (radius ≤ 0.3). The iteration stopped whenever $\|z\| > 0.4$ or the number of iterations reached a maximum value (1000).

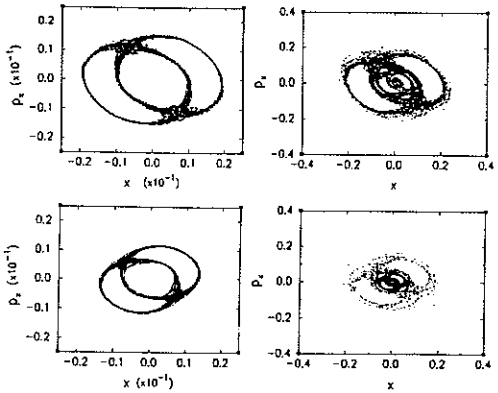

FIG. 2. Poincaré sections of f_E (F_E), for $E = 0.1666666667$ are shown on the top (bottom), for $b = 0.40$ (left) and $b = 0.48$ (right). Initial conditions were taken on the axes x and p_x, within a radius of 0.01 (0.013) for f_E (F_E). Notice the factor of 10 between the scales used for the two b values considered.

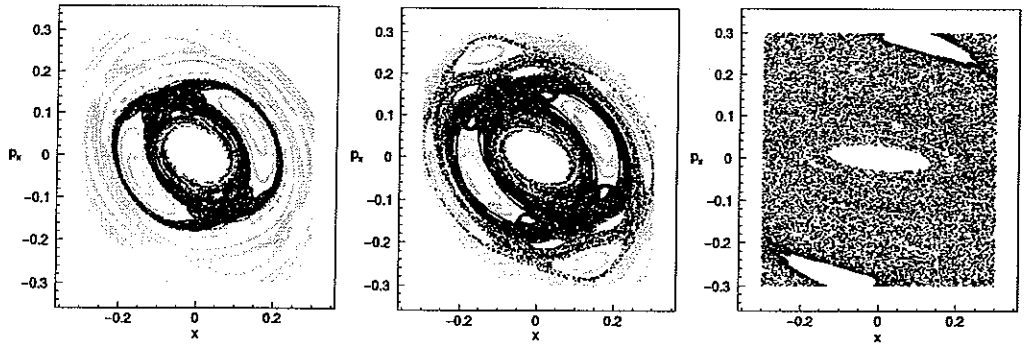

FIG. 3. Poincaré sections of f_E for $E = 0.17$, and $b = 0.40, 0.48, 1.0$ from left to right. The black dots correspond to orbits that escape and grey dots to orbits that do not escape. Points falling inside the central white circle escape immediatly.